XLIII CILAMCE
21–25, November, 2022
FOZ DO IGUAÇU – PR – BRAZIL

Wavefront velocity for foam flow in three-layer porous media

A. J. Castrillón Vásquez [a,b,1], G. Chapiro[a,2]

[a] *Laboratory of Applied Mathematics, Federal University of Juiz de Fora, Brazil*
[b] *Computational Modeling Graduate Program, Federal University of Juiz de Fora, Brazil*
[1] *andresjulian@ice.ufjf.br*
[2] *grigori@ice.ufjf.br*

Abstract. The foam became interesting for many applications, including the oil industry, due to its capacity to control gas mobility, which is specifically relevant in fractured reservoirs. In the present work, we use a simplified bubble population balance model to describe foam displacement in porous media. We approach the fractured structure of the porous medium in a three-layer configuration, where the middle layer possesses a small width and high permeability. Numerical investigation using Foam Displacement Simulator (FOSSIL) points out the existence of a stable traveling wave water saturation profile evidencing the applicability of the foam injection to control gas mobility in fractured reservoirs.

Keywords: Traveling waves, Foam flow, Multilayer, Porous medium

1 Introduction

There is a growing interest in studying the foam displacement in porous media, from an environmental (soil remediation) as shown in Bertin et al. [1], or industrial (oil recovery) point of view as in Hematpur et al. [2]. Several models describe the behavior of foam in porous media, see Ashoori et al. [3], Kovscek et al. [4], Kam et al. [5]. Within these models are local equilibrium models and population balance models see Hematpur et al. [2]. We are interested in the latter, where the foam texture is modeled using the mass balance equation. These models are more realistic as they consider physical aspects of foam creation and destruction.

There are some studies of multiphase flow in porous media by layers; see Leij et al. [6], Guerrero et al.[7], Worthy et al.[8], Carr et al. [9] and Kumar et al. [10]. Some of them, i.e., Guerrero et al. [7] use Laplace transform to estimate the analytical solutions; others Kumar et al. [10] consider fractures between the layers and study the multiphase flow when the fracture thickness tends to zero. In the case of foam displacement, one can find articles, such as Bertin et al. [1], where artificial media with different permeabilities but the same porosity in each layer are studied for soil remediation. The behavior of multiphase flow with the presence of foam is explored in Li et al. [11] in the context of microfluidics. In Rosman et al. [12], the velocities and saturations of water in two-layer porous media with different permeabilities, but equal porosity, are analyzed from the computational point of view.

Using the linear kinetic model Ashoori et al. [3] in the previous work by Castrillon et al. [13], the problem of foam flow in two-layer media is investigated using traveling waves; the velocity of this wave was found. This paper proposes an extension of this study to the three-layer case using the bubble balance population foam model from Zitha et al. [14] with simplifying hypothesis of Newtonian flow as in Zavala et al. [15]. We use 2D simulations to show the existence of the traveling wave solution profile.

This paper is structured as follows. Section 2 presents the simplified version of the bubble population model, see [14]. In section 3, we describe Foam Displacement Simulator (FOSSIL) (see De Paula et al. [16]), and the main numerical results. In section 4, we summarize the conclusions, highlighting the importance of the study of foam flow in porous media.

2 Model

Based on De Paula [16], and Castrillon et al. [13], we consider the following system of partial differential equations, which describes the two-dimensional foam displacement in porous media

$$\begin{cases} \phi \frac{\partial}{\partial t} S_{\mathrm{w}} + \nabla \cdot u_{\mathrm{w}} &= 0, \\ \phi \frac{\partial}{\partial t}(n_{\mathrm{D}} S_{\mathrm{g}}) + \nabla \cdot (u_{\mathrm{g}} n_{\mathrm{D}}) &= \phi S_{\mathrm{g}} \Phi \,, \end{cases} \tag{1}$$

where ϕ is the porosity, S_{w} is the water saturation, u_{w} is the water velocity, n_{D} is the foam texture, S_{g} is the gas saturation, u_{g} is the gas velocity, and Φ represents the foam generation and coalescence. The first equation in (1) is a conservation law, while the second equation in (1) is a population balance equation considering $u = u_{\mathrm{w}} + u_{\mathrm{g}}$ as Darcy's velocity

$$u_w = -\lambda_{\mathrm{w}} \nabla P_w, \tag{2}$$

where λ_{w} is the mobility of water phase and P_w is the pressure in the water phase. The two-dimensional domain for eq. (1) is the rectangle $\Omega := (0, L) \times (-d, d_3)$ (see Fig.1), where L is the maximum length in the axis x and the height z is in $(-d, d_3)$. We solve the problem in three layers of different permeability: the first $z \in (-d, d_1)$ with permeability $k = k_1$ and porosity ϕ, the second with $z \in (d_1, d_2)$ permeability $k = k_2$, porosity ϕ; and the third with $z \in (d_2, d_3)$ $k = k_3$, porosity ϕ.

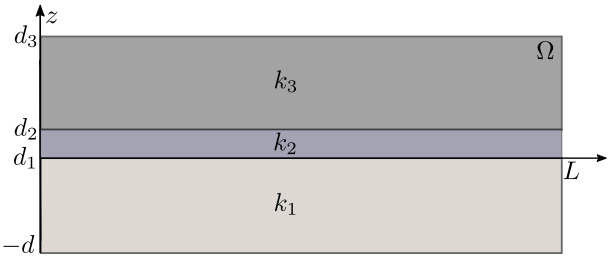

Figure 1. Schematic representation of a three-layered porous medium as a domain $\Omega := (0, L) \times (-d, d_3)$; where, k_i is the permeabilities of the layer i, respectively.

We use the stochastic population model given in Zitha et al.[14] with the simplification proposed in Zavala et al. [15] to define the foam generation source term as:

$$\Phi = (K_c + K_g)(n_{\mathrm{D}}^{\mathrm{LE}} - n_{\mathrm{D}}), \tag{3}$$

which depends on foam texture in local equilibrium $n_{\mathrm{D}}^{\mathrm{LE}}(S_{\mathrm{w}})$ given by:

$$n_{\mathrm{D}}^{\mathrm{LE}}(S_{\mathrm{w}}) = \frac{K_g}{K_c + K_g}, \tag{4}$$

where K_g and K_c are the coalescence coefficients given in Zitha et al. [17]. Considering the fractional flow function theory from Ashoori et al. [3], Persoff et al.[18], Zitha et al. [19], and Zavala et al.[15],

$$\lambda_{\mathrm{w}} = k\frac{k_{\mathrm{rw}}}{\mu_{\mathrm{w}}}, \;\; \lambda_{\mathrm{g}} = k\frac{k_{\mathrm{rg}}}{\mu_{\mathrm{g}}}, \;\; f_{\mathrm{w}} = \frac{\lambda_{\mathrm{w}}}{\lambda_{\mathrm{w}} + \lambda_{\mathrm{g}}}, \;\; f_{\mathrm{g}} = \frac{\lambda_{\mathrm{g}}}{\lambda_{\mathrm{w}} + \lambda_{\mathrm{g}}}, \tag{5}$$

where λ is a modified pore-size distribution parameter, λ_{w} and λ_{g} are the mobilities of water and gas phases; μ_{w} and μ_g are the viscosity parameters for water and gas phases, f_{w} and f_{g} are fractional flows for water and gas phases. As the system is entirely saturated we consider that $S_{\mathrm{w}} + S_{\mathrm{g}} = 1$ and $f_{\mathrm{w}} + f_{\mathrm{g}} = 1$. The partial mobilities and fractional flow functions can be defined as:

$$k_{\mathrm{rw}}(S_{\mathrm{w}}) = \begin{cases} 0, & 0 \le S_{\mathrm{w}_i} \le S_{\mathrm{wc}}, \\ 0.75 \left(\dfrac{S_{\mathrm{w}} - S_{\mathrm{wc}}}{1 - S_{\mathrm{wc}} - S_{\mathrm{gr}}} \right)^{\lambda}, & S_{\mathrm{wc}} < S_{\mathrm{w}} \le 1, \end{cases} \tag{6}$$

$$k_{\mathrm{rg}}^0(S_{\mathrm{w}}) = \begin{cases} 0.94 \left(\dfrac{1 - S_{\mathrm{w}} - S_{\mathrm{gr}}}{1 - S_{\mathrm{wc}} - S_{\mathrm{gr}}} \right)^{(3\lambda+2)/\lambda}, & 0 \le S_{\mathrm{w}} < 1 - S_{\mathrm{gr}}, \\ 0, & 1 - S_{\mathrm{gr}} \le S_{\mathrm{w}_i} \le 1. \end{cases} \tag{7}$$

Table 1. Parameter values for the problem of three layers.

Symbol	Value	Parameter
S_{wc}	0.2 [-]	connate water saturation
S_{gr}	0.0 [-]	residual gas saturation
μ_w	10^{-3} $[Pa\,s]$	water viscosity
μ_g^0	$2 \cdot 10^{-5}$ $[Pa\,s]$	gas viscosity in absence of foam
k_1	$1 \cdot 10^{-12}$ $[m^2]$	permeability of medium in layer 1
k_2	$1 \cdot 10^{-11}$ $[m^2]$	permeability of medium in layer 2
k_3	$1 \cdot 10^{-12}$ $[m^2]$	permeability of medium in layer 3
$n_{\max}$	$2.5 \cdot 10^{11}$ $[m^{-3}]$	maximum foam texture
u	$2.31 \cdot 10^{-5}$ $[ms^{-1}]$	average total velocity
K_C	0 $[s^{-1}]$	bubble coalescence coefficient
K_g	0.1 $[s^{-1}]$	bubble generation coefficient
λ	5 [-]	pore-size distribution parameter
ϕ	0.21 [-]	porosity
$S_{\text{w}_i}^+$	0.99[-]	inicial water saturation for the layer i, $i = 1, 2, 3$
$S_{\text{w}_i}^-$	0.63[-]	injected water saturation for the layer i, $i = 1, 2, 3$
σ_{gm}	$30 \cdot 10^{-3}$ $[N/m]$	gas-water interfacial tension
α	$5.8 \cdot 10^{-16}$ $[Pa\,s^{2/3}\,m^{10/3}]$	viscosity proportionality constant
r	$5 \cdot 10^{-6}[m]$	mean pore radius
D	0.02 $[m]$	constant to define the thickness of the layers

$$k_{\text{rg}}(S_{\text{w}}, n_{\text{D}}) = \frac{k_{\text{rg}}^0(S_{\text{w}})}{MRF(n_{\text{D}})}, \tag{8}$$

the gas mobility reduction factor ($MRF = \mu_f/\mu_g^0$), where μ_f is the viscosity of the flowing gas and μ_g^0 the viscosity in the absence of foam, could be seen as a linear function of foam texture:

$$MRF(n_{\text{D}}) = \beta n_{\max} n_{\text{D}} + 1. \tag{9}$$

where

$$\beta = \frac{\alpha}{(u_{\text{g}}/\phi S_{\text{g}}))^d\, \mu_g^0}. \tag{10}$$

The capillary-pressure P_c is a function depending on S_{w}, and on the gas-water surface tension σ, on the porosity of medium ϕ and permeability k is defined as:

$$P_c = p_{c,0} \cdot \gamma \cdot \left(\frac{S_{\text{w}} - S_{\text{wc}}}{0.5 - S_{\text{wc}}} \right)^{-1/\lambda}, \tag{11}$$

considering $p_{c,0} = 2\,(\sigma_{gw}/r)\,cos\theta$ as the entry capillarity pressure, γ is the proportionality coefficient, σ_{gw} is the surface tension between water and gas, θ is the contact angle, and r is the effective pore radius. All the parameters mentioned so here, can be seen in Table (1).

3 Numerical Results

In this section, we show the results obtained for a 2D model using Foam Displacement Simulator (FOSSIL), whose detailed description can be found in De Paula et al. [16]. To solve the problem composed of the first

equation in (1) and eq.(2), FOSSIL uses the conservative mixed finite element method proposed in Kurganov et al. [20]. To solve the second equation of (1) (which corresponds to the foam transport problem), FOSSIL uses the conservative method KNP introduced in Kurganov et al. [21], which is an extension of the finite volume method presented in Kurgarov et al. [22].

To obtain the solutions of the problem (1) we use 2D simulations with the following conditions in the domain Ω (depicted in Fig. 2): At $x = 0$, we consider a constant velocity for all z, and the water saturation S_{w} equal to the injection condition $S_{\text{w}} = S_{\text{w}}^{-}$. At $x = L$, we consider the Newmann type boundary condition $\partial_x S_{\text{w}} = 0$. The permeability of the medium k is a matrix of dimension $m \times n_z$, where m is the number of cells on the horizontal axis, and n_z is the same on the vertical axis (we consider n_z multiple of 21). It is defined as:

$$k_{ij} = \begin{cases} k_1, & \text{if } j \in [1, (3/7)n_z] \cap \mathbb{Z}, \\ k_2, & \text{if } j \in [(10/21)n_z, (11/21)n_z] \cap \mathbb{Z}, \\ k_3, & \text{if } j \in [(4/7)n_z, n_z] \cap \mathbb{Z}. \end{cases} \tag{12}$$

A graphical representation of how permeability is defined over the entire domain is shown in Fig. 2, where Δz represents the cell width in z direction, Δx is the cell width in x direction. For this experiment, $|d_2 - d_3| = |-d - d_1| = D$ and $|d_2 - d_1| = (1/10)D$, where D is given in Table 1.

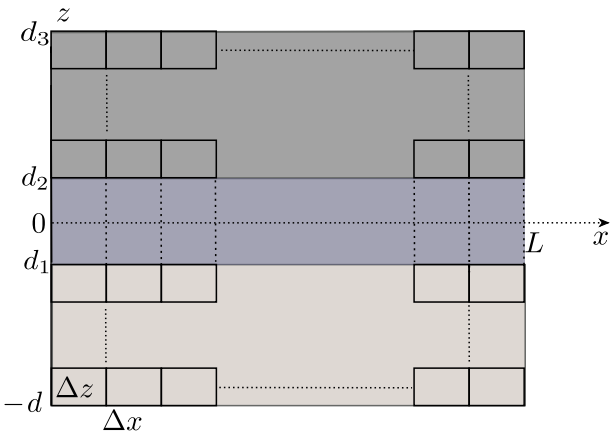

Figure 2. Numerical domain for the three-layer problem.

Figure 3 shows the behavior of the water saturation in the whole domain at three different times. Simulation results in Fig. 3 indicate the presence of the stable traveling wave saturation profile. This behavior is similar to one described in Zavala et al. [15] for the one-dimensional case.

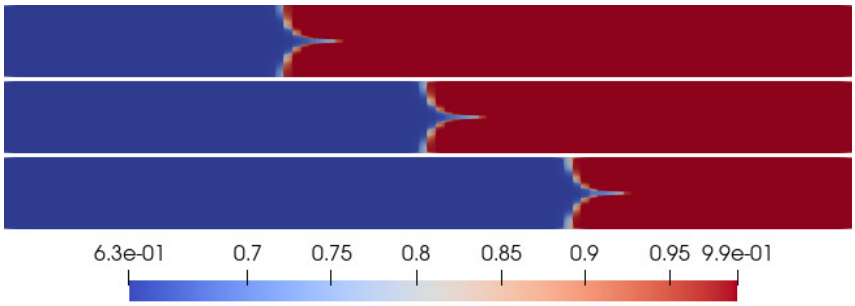

Figure 3. Stable traveling water saturation profile obtained through two-dimensional numerical simulations at $2500\,s$ (upper plot), $3750\,s$ (middle plot) and $5000\,s$ (lower plot).

To calculate the position of the water saturation wavefront, shown in Fig. 4, we modify the algorithm proposed in Castrillon et al. [13] given below. The position x_i^{front} with $i = 1, 2, 3$ is calculated using:

$$x_1^{front} = \underset{i=1\cdots(9/21)n_z}{\text{mean}} x_{\text{strip}\,i}^{\text{front}}, \tag{13}$$

$$x_2^{front} = \underset{i=(10/21)n_z\cdots(11/21)n_z}{\text{mean}} x_{\text{strip}\,i}^{\text{front}}, \tag{14}$$

$$x_3^{front} = \underset{i=(12/21)n_z\cdots n_z}{\text{mean}} x_{\text{strip}\,i}^{\text{front}}. \tag{15}$$

Using equations (13)-(15) and finite differences, we calculate the wave velocity in each layer i in a similar way as it is done in Castrillon et al. [13]:

$$v_{i,k} = \frac{x_{i,k}^{front} - x_{i,k-1}^{front}}{\Delta t}. \tag{16}$$

Figures 4 and 5b show that the wave in the middle layer moves faster than in the other two layers for times shorter

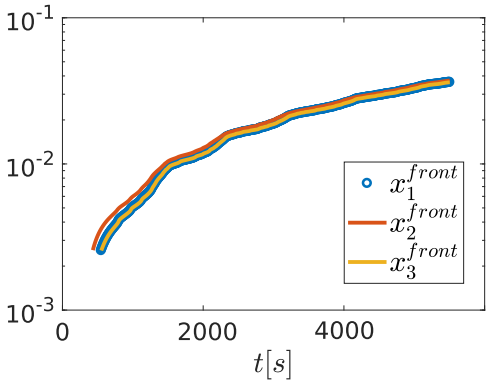

Figure 4. Position on the horizontal axis of the water saturation front x_i^{front} in each of the i-layers.

than $2000\,s$. After this time, the saturation fronts move at the same velocity. Figure 6 presents saturation profiles obtained numerically at different times starting with $t = 2500\,s$. In this figure, we also show the displaced initial profile comparing $S_{\mathrm{w}} + v\Delta t$ with $S_{\mathrm{w}}(t + \Delta t)$, where v is the stable velocity in different layers. We estimate the velocity v using the moving average with groups of 300 points obtained with a numerical approximation of the traveling wave velocity. The final value of v is the the arithmetic average of the regularized velocities from $t = 3000\,s$ until $t = 10.000\,s$. As one can observe, after the stabilization time (see Fig. 5b and 5a), the water saturation profiles move with constant velocity v without changing the wave shape.

The proximity of the curves $S_{\mathrm{w}} + v\Delta t$ with $S_{\mathrm{w}}(t + \Delta t)$ in Fig. 6, can be quantified using the L^2 distance, see results in Table 2. As we can observe, the distance between the profiles does not increase over time, corroborating the existence of a traveling wave solution connecting S_{w}^- to S_{w}^+.

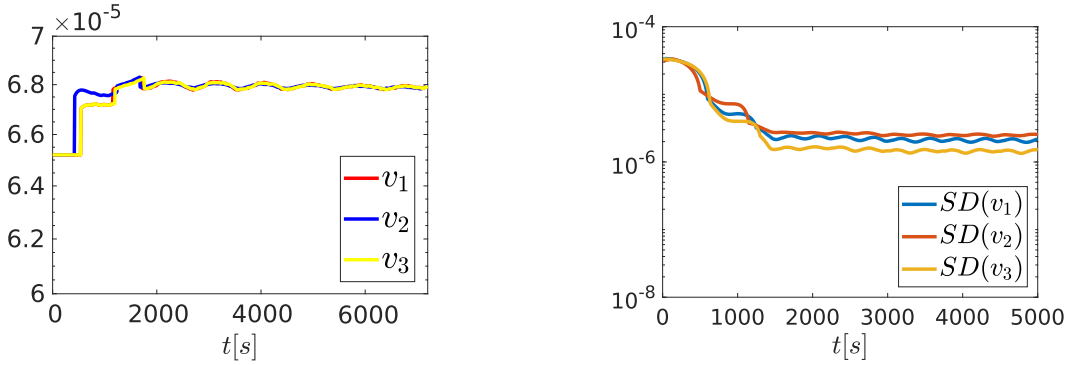

(a) Velocities for each layer

(b) Standard deviation of speeds

Figure 5. Velocities v_i in the layer i; and standard deviation of each velocity $SD(v_i)$ in the layer i. Simulated using the moving average for groups of 240 data in the 2D-model.

4 Conclusions

In this work, we investigated the foam displacement in three-layer stratified porous media using the bubble population model. Using the in-house numerical simulator in the two-dimensional configuration, we conclude that the water saturation profile behaves as a stable traveling wave solution. As a highly permeable middle layer can approach fracture, our results indicate that the foam displacement in the porous media containing fractures presents a behavior similar to that observed in the homogeneous case.

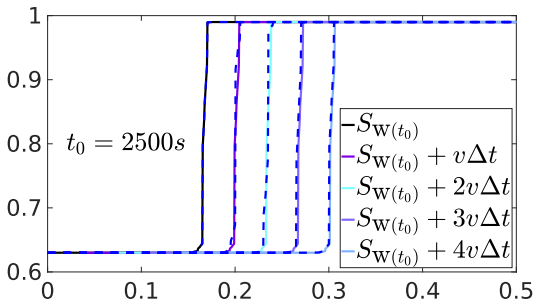

(a) Layer 1

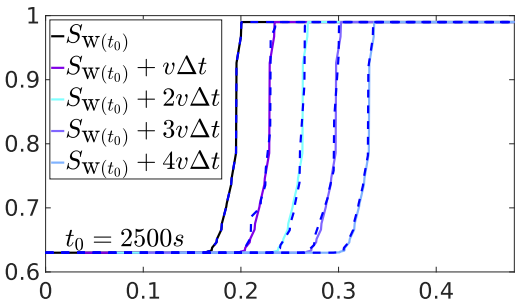

(b) Layer 2

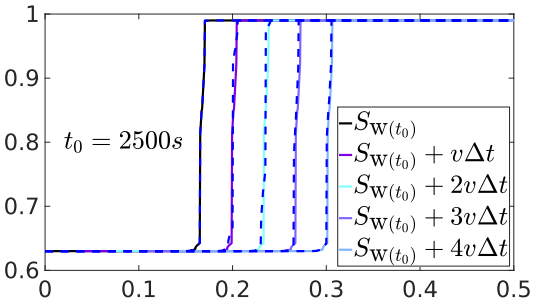

(c) Layer 3

Figure 6. Comparison of the profiles using the calculated velocity $v = 6.8e \times 10^{-5} m/s$. The dotted curves are generated by FOSSIL at times $t_0 = 2500s$, $t_1 = 3000s$, $t_2 = 3500s$, $t_3 = 4000s$, and $t_4 = 4500s$. S_{w_0} is the profile generated by FOSSIL at time $2500s$. (a) In layer 1, (b) layer 2 and (c) layer 3. The distance between $S_{w_0} + v\Delta t$ and $S_w(t)$ are shown in Table 2.

Table 2. Distance between $S_w(2500) + v\Delta t$ and $S_w(2500 + \Delta t)$ in the layer i.

Δt	Layer 1	Layer 2	Layer 3
500 s	8.3e-3	3e-3	8.3e-3
1000 s	2.02e-3	4.8e-3	2.08e-3
1500 s	1.6e-3	1.3e-3	1.7e-3
2000 s	2e-3	2.3e-3	2.02e-3

Acknowledgements. The current work was conducted in association with the R&D projects ANP n° 20715-9, "Modelagem matemática e computacional de injeção de espuma usada em recuperação avançada de petróleo" (UFJF/Shell Brazil/ANP). Shell Brazil funds it in accordance with ANP's R&D regulations under the Research, Development, and Innovation Investment Commitment. This project is carried out in partnership with Petrobras.

G. Chapiro was supported in part by CNPq grants 303245/2019-0 and 405366/2021-3, and FAPEMIG grant APQ-00405-21.

Authorship statement. The authors hereby confirm that they are the sole liable persons responsible for the authorship of this work, and that all material that has been herein included as part of the present paper is either the property (and authorship) of the authors, or has the permission of the owners to be included here.

References

[1] H. Bertin, E. Estrada, and O. Atteia. Foam placement for soil remediation. *Environ. Chem.*, vol. 14, pp. 338–343, 2017.

[2] H. Hematpur, S. M. Mahmood, N. H. Nasr, and K. A. Elraies. Foam flow in porous media: Concepts, models and challenges. *Journal of Natural Gas Science and Engineering*, vol. 53, pp. 163–180, 2018.

[3] E. Ashoori, D. Marchesin, and W. R. Rossen. Roles of transient and local equilibrium foam behavior in porous media: traveling wave. *Colloids and Surfaces A: Physicochemical and Engineering Aspects*, vol. 377, pp.

228–242, 2011.
[4] A. R. Kovscek, T. W. Patzek, and C. J. Radke. A mechanistic population balance model for transient and steady-state foam flow in Boise sandstone. *Chemical Engineering Science*, vol. 50, n. 23, pp. 3783–3799, 1995.
[5] S. I. Kam, Q. P. Nguyen, Q. Li, and W. R. Rossen. Dynamic simulations with an improved model for foam generation. *SPE Journal*, vol. 12, n. 1, pp. 35–48, 2007.
[6] F. J. Leij and M. T. Van Genuchten. Approximate analytical solutions for solute transport in two-layer porous media. *Transport in Porous Media*, vol. 18, n. 1, pp. 65–85, 1995.
[7] J. S. P. Guerrero, L. C. G. Pimentel, and T. H. Skaggs. Analytical solution for the advection-dispersion transport equation in layered media. *Heat Mass Transf*, vol. 56, pp. 274–282, 2013.
[8] M. R. Rodrigo and A. L. Worthy. Solution of multilayer diffusion problems via the laplace transform. *J. Math. Anal. Appl*, vol. 444, pp. 475–502, 2016.
[9] E. J. Carr and I. W. Turner. A semi-analytical solution for multilayer diffusion in a composite medium consisting of a large number of layers. *Appl. Math. Model*, vol. 40, pp. 7034–7050, 2016.
[10] K. Kumar, F. List, I. S. Pop, and F. A. Radu. Formal upscaling and numerical validation of unsaturated flow models in fractured porous media. *Journal of Computational Physics*, vol. 407, pp. 109138, 2020.
[11] Q. Li and W. R. Rossen. Injection Strategies for Foam Generation in Homogeneous and Layered Porous Media. In *SPE Annual Technical Conference and Exhibition*. Society of Petroleum Engineers, 2005.
[12] A. Rosman and S. I. Kam. Modeling foam-diversion process using three-phase fractional flow analysis in a layered system. *Energy Sources, Part A: Recovery, Utilization, and Environmental Effects*, vol. 31, n. 11, pp. 936–955, 2009.
[13] A. J. C. Vasquez, L. F. Lozano, W. Pereira, J. B. Cedro, and G. Chapiro. The traveling wavefront for foam flow in two-layer porous media. *submitted*, vol. , 2022.
[14] P. L. J. Zitha and D. X. Du. A new stochastic bubble population model for foam flow in porous media. *Transport in Porous Media*, vol. 83, n. 3, pp. 603–621, 2010.
[15] R. Q. Zavala, L. F. Lozano, P. L. J. Zitha, and G. Chapiro. Analytical solution for the population-balance model describing foam displacement. *Transport in Porous Media*, vol. , pp. 1–17, 2021.
[16] F. F. de Paula, T. Quinelato, I. Igreja, and G. Chapiro. A numerical algorithm to solve the two-phase flow in porous media including foam displacement. In *Lecture Notes in Computer Science*, volume 12143, pp. 18–31. Springer, 2020.
[17] P. L. J. Zitha. A new stochastic bubble population model for foam in porous media. In *SPE/DOE Symposium on Improved Oil Recovery*. Society of Petroleum Engineers, 2006.
[18] P. Persoff, C. J. Radke, K. Pruess, S. M. Benson, and P. A. Witherspoon. A laboratory investigation of foam flow in sandstone at elevated pressure. In *SPE California Regional Meeting*. Society of Petroleum Engineers, 1989.
[19] P. L. J. Zitha, Q. P. Nguyen, P. K. Currie, and M. A. Buijse. Coupling of foam drainage and viscous fingering in porous media revealed by X-ray computed tomography. *Transport in Porous Media*, vol. 64, n. 3, pp. 301–313, 2006.
[20] A. Kurganov, Z. Qu, O. S. Rozanova, and T. Wu. Adaptive moving mesh central-upwind schemes for hyperbolic system of PDEs: Applications to compressible Euler equations and granular hydrodynamics. *Communications on Applied Mathematics and Computation*, vol. 3, n. 3, pp. 445–479, 2021.
[21] A. Kurganov, S. Noelle, and G. Petrova. Semidiscrete central-upwind schemes for hyperbolic conservation laws and Hamilton-Jacobi equations. *SIAM Journal on Scientific Computing*, vol. 23, n. 3, pp. 707–740, 2001.
[22] A. Kurganov and E. Tadmor. New high-resolution central schemes for nonlinear conservation laws and convection-diffusion equations. *Journal of Computational Physics*, vol. 160, n. 1, pp. 241–282, 2000.